Measurement of the $B^0 \to J/\psi\pi^+\pi^-$ Branching Fraction

B. Aubert,[1] D. Boutigny,[1] J.-M. Gaillard,[1] A. Hicheur,[1] Y. Karyotakis,[1] J. P. Lees,[1] P. Robbe,[1] V. Tisserand,[1] A. Zghiche,[1] A. Palano,[2] A. Pompili,[2] J. C. Chen,[3] N. D. Qi,[3] G. Rong,[3] P. Wang,[3] Y. S. Zhu,[3] G. Eigen,[4] I. Ofte,[4] B. Stugu,[4] G. S. Abrams,[5] A. W. Borgland,[5] A. B. Breon,[5] D. N. Brown,[5] J. Button-Shafer,[5] R. N. Cahn,[5] E. Charles,[5] M. S. Gill,[5] A. V. Gritsan,[5] Y. Groysman,[5] R. G. Jacobsen,[5] R. W. Kadel,[5] J. Kadyk,[5] L. T. Kerth,[5] Yu. G. Kolomensky,[5] J. F. Kral,[5] C. LeClerc,[5] M. E. Levi,[5] G. Lynch,[5] L. M. Mir,[5] P. J. Oddone,[5] T. J. Orimoto,[5] M. Pripstein,[5] N. A. Roe,[5] A. Romosan,[5] M. T. Ronan,[5] V. G. Shelkov,[5] A. V. Telnov,[5] W. A. Wenzel,[5] T. J. Harrison,[6] C. M. Hawkes,[6] D. J. Knowles,[6] S. W. O'Neale,[6] R. C. Penny,[6] A. T. Watson,[6] N. K. Watson,[6] T. Deppermann,[7] K. Goetzen,[7] H. Koch,[7] B. Lewandowski,[7] K. Peters,[7] H. Schmuecker,[7] M. Steinke,[7] N. R. Barlow,[8] W. Bhimji,[8] J. T. Boyd,[8] N. Chevalier,[8] P. J. Clark,[8] W. N. Cottingham,[8] C. Mackay,[8] F. F. Wilson,[8] K. Abe,[9] C. Hearty,[9] T. S. Mattison,[9] J. A. McKenna,[9] D. Thiessen,[9] S. Jolly,[10] A. K. McKemey,[10] V. E. Blinov,[11] A. D. Bukin,[11] A. R. Buzykaev,[11] V. B. Golubev,[11] V. N. Ivanchenko,[11] A. A. Korol,[11] E. A. Kravchenko,[11] A. P. Onuchin,[11] S. I. Serednyakov,[11] Yu. I. Skovpen,[11] A. N. Yushkov,[11] D. Best,[12] M. Chao,[12] D. Kirkby,[12] A. J. Lankford,[12] M. Mandelkern,[12] S. McMahon,[12] D. P. Stoker,[12] K. Arisaka,[13] C. Buchanan,[13] S. Chun,[13] D. B. MacFarlane,[14] S. Prell,[14] Sh. Rahatlou,[14] G. Raven,[14] V. Sharma,[14] J. W. Berryhill,[15] C. Campagnari,[15] B. Dahmes,[15] P. A. Hart,[15] N. Kuznetsova,[15] S. L. Levy,[15] O. Long,[15] A. Lu,[15] M. A. Mazur,[15] J. D. Richman,[15] W. Verkerke,[15] J. Beringer,[16] A. M. Eisner,[16] M. Grothe,[16] C. A. Heusch,[16] W. S. Lockman,[16] T. Pulliam,[16] T. Schalk,[16] R. E. Schmitz,[16] B. A. Schumm,[16] A. Seiden,[16] M. Turri,[16] W. Walkowiak,[16] D. C. Williams,[16] M. G. Wilson,[16] E. Chen,[17] G. P. Dubois-Felsmann,[17] A. Dvoretskii,[17] D. G. Hitlin,[17] F. C. Porter,[17] A. Ryd,[17] A. Samuel,[17] S. Yang,[17] S. Jayatilleke,[18] G. Mancinelli,[18] B. T. Meadows,[18] M. D. Sokoloff,[18] T. Barillari,[19] P. Bloom,[19] W. T. Ford,[19] U. Nauenberg,[19] A. Olivas,[19] P. Rankin,[19] J. Roy,[19] J. G. Smith,[19] W. C. van Hoek,[19] L. Zhang,[19] J. Blouw,[20] J. L. Harton,[20] M. Krishnamurthy,[20] A. Soffer,[20] W. H. Toki,[20] R. J. Wilson,[20] J. Zhang,[20] D. Altenburg,[21] T. Brandt,[21] J. Brose,[21] T. Colberg,[21] M. Dickopp,[21] R. S. Dubitzky,[21] A. Hauke,[21] E. Maly,[21] R. Müller-Pfefferkorn,[21] S. Otto,[21] K. R. Schubert,[21] R. Schwierz,[21] B. Spaan,[21] L. Wilden,[21] D. Bernard,[22] G. R. Bonneaud,[22] F. Brochard,[22] J. Cohen-Tanugi,[22] S. Ferrag,[22] S. T'Jampens,[22] Ch. Thiebaux,[22] G. Vasileiadis,[22] M. Verderi,[22] A. Anjomshoaa,[23] R. Bernet,[23] A. Khan,[23] D. Lavin,[23] F. Muheim,[23] S. Playfer,[23] J. E. Swain,[23] J. Tinslay,[23] M. Falbo,[24] C. Borean,[25] C. Bozzi,[25] L. Piemontese,[25] A. Sarti,[25] E. Treadwell,[26] F. Anulli,[27,*] R. Baldini-Ferroli,[27] A. Calcaterra,[27] R. de Sangro,[27] D. Falciai,[27] G. Finocchiaro,[27] P. Patteri,[27] I. M. Peruzzi,[27,*] M. Piccolo,[27] A. Zallo,[27] S. Bagnasco,[28] A. Buzzo,[28] R. Contri,[28] G. Crosetti,[28] M. Lo Vetere,[28] M. Macri,[28] M. R. Monge,[28] S. Passaggio,[28] F. C. Pastore,[28] C. Patrignani,[28] E. Robutti,[28] A. Santroni,[28] S. Tosi,[28] M. Morii,[29] R. Bartoldus,[30] G. J. Grenier,[30] U. Mallik,[30] J. Cochran,[31] H. B. Crawley,[31] J. Lamsa,[31] W. T. Meyer,[31] E. I. Rosenberg,[31] J. Yi,[31] M. Davier,[32] G. Grosdidier,[32] A. Höcker,[32] H. M. Lacker,[32] S. Laplace,[32] F. Le Diberder,[32] V. Lepeltier,[32] A. M. Lutz,[32] T. C. Petersen,[32] S. Plaszczynski,[32] M. H. Schune,[32] L. Tantot,[32] S. Trincaz-Duvoid,[32] G. Wormser,[32] R. M. Bionta,[33] V. Brigljević,[33] D. J. Lange,[33] M. Mugge,[33] K. van Bibber,[33] D. M. Wright,[33] A. J. Bevan,[34] J. R. Fry,[34] E. Gabathuler,[34] R. Gamet,[34] M. George,[34] M. Kay,[34] D. J. Payne,[34] R. J. Sloane,[34] C. Touramanis,[34] M. L. Aspinwall,[35] D. A. Bowerman,[35] P. D. Dauncey,[35] U. Egede,[35] I. Eschrich,[35] G. W. Morton,[35] J. A. Nash,[35] P. Sanders,[35] D. Smith,[35] G. P. Taylor,[35] J. J. Back,[36] G. Bellodi,[36] P. Dixon,[36] P. F. Harrison,[36] R. J. L. Potter,[36] H. W. Shorthouse,[36] P. Strother,[36] P. B. Vidal,[36] G. Cowan,[37] H. U. Flaecher,[37] S. George,[37] M. G. Green,[37] A. Kurup,[37] C. E. Marker,[37] T. R. McMahon,[37] S. Ricciardi,[37] F. Salvatore,[37] G. Vaitsas,[37] M. A. Winter,[37] D. Brown,[38] C. L. Davis,[38] J. Allison,[39] R. J. Barlow,[39] A. C. Forti,[39] F. Jackson,[39] G. D. Lafferty,[39] N. Savvas,[39] J. H. Weatherall,[39] J. C. Williams,[39] A. Farbin,[40] A. Jawahery,[40] V. Lillard,[40] D. A. Roberts,[40] J. R. Schieck,[40] G. Blaylock,[41] C. Dallapiccola,[41] K. T. Flood,[41] S. S. Hertzbach,[41] R. Kofler,[41] V. B. Koptchev,[41] T. B. Moore,[41] H. Staengle,[41] S. Willocq,[41] B. Brau,[42] R. Cowan,[42] G. Sciolla,[42] F. Taylor,[42] R. K. Yamamoto,[42] M. Milek,[43] P. M. Patel,[43] F. Palombo,[44] J. M. Bauer,[45] L. Cremaldi,[45] V. Eschenburg,[45] R. Kroeger,[45] J. Reidy,[45] D. A. Sanders,[45] D. J. Summers,[45] C. Hast,[46] P. Taras,[46] H. Nicholson,[47] C. Cartaro,[48] N. Cavallo,[48] G. De Nardo,[48] F. Fabozzi,[48] C. Gatto,[48] L. Lista,[48] P. Paolucci,[48] D. Piccolo,[48] C. Sciacca,[48] J. M. LoSecco,[49] J. R. G. Alsmiller,[50] T. A. Gabriel,[50] J. Brau,[51] R. Frey,[51] M. Iwasaki,[51] C. T. Potter,[51] N. B. Sinev,[51] D. Strom,[51] E. Torrence,[51] F. Colecchia,[52] A. Dorigo,[52] F. Galeazzi,[52] M. Margoni,[52] M. Morandin,[52] M. Posocco,[52] M. Rotondo,[52] F. Simonetto,[52] R. Stroili,[52] C. Voci,[52] M. Benayoun,[53] H. Briand,[53] J. Chauveau,[53] P. David,[53] Ch. de la Vaissière,[53] L. Del Buono,[53] O. Hamon,[53] Ph. Leruste,[53] J. Ocariz,[53] M. Pivk,[53] L. Roos,[53] J. Stark,[53] P. F. Manfredi,[54] V. Re,[54] V. Speziali,[54] L. Gladney,[55] Q. H. Guo,[55] J. Panetta,[55] C. Angelini,[56] G. Batignani,[56] S. Bettarini,[56] M. Bondioli,[56] F. Bucci,[56] G. Calderini,[56] E. Campagna,[56] M. Carpinelli,[56] F. Forti,[56] M. A. Giorgi,[56] A. Lusiani,[56] G. Marchiori,[56]

 0031-9007/03/90(9)/091801(7)$20.00

F. Martinez-Vidal,[56] M. Morganti,[56] N. Neri,[56] E. Paoloni,[56] M. Rama,[56] G. Rizzo,[56] F. Sandrelli,[56] G. Triggiani,[56] J. Walsh,[56] M. Haire,[57] D. Judd,[57] K. Paick,[57] L. Turnbull,[57] D. E. Wagoner,[57] J. Albert,[58] P. Elmer,[58] C. Lu,[58] V. Miftakov,[58] J. Olsen,[58] S. F. Schaffner,[58] A. J. S. Smith,[58] A. Tumanov,[58] E. W. Varnes,[58] F. Bellini,[59] G. Cavoto,[58,59] D. del Re,[14,59] R. Faccini,[14,59] F. Ferrarotto,[59] F. Ferroni,[59] E. Leonardi,[59] M. A. Mazzoni,[59] S. Morganti,[59] G. Piredda,[59] F. Safai Tehrani,[59] M. Serra,[59] C. Voena,[59] S. Christ,[60] G. Wagner,[60] R. Waldi,[60] T. Adye,[61] N. De Groot,[61] B. Franek,[61] N. I. Geddes,[61] G. P. Gopal,[61] S. M. Xella,[61] R. Aleksan,[62] S. Emery,[62] A. Gaidot,[62] P.-F. Giraud,[62] G. Hamel de Monchenault,[62] W. Kozanecki,[62] M. Langer,[62] G. W. London,[62] B. Mayer,[62] G. Schott,[62] B. Serfass,[62] G. Vasseur,[62] Ch. Yeche,[62] M. Zito,[62] M. V. Purohit,[63] A. W. Weidemann,[63] F. X. Yumiceva,[63] I. Adam,[64] D. Aston,[64] N. Berger,[64] A. M. Boyarski,[64] M. R. Convery,[64] D. P. Coupal,[64] D. Dong,[64] J. Dorfan,[64] W. Dunwoodie,[64] R. C. Field,[64] T. Glanzman,[64] S. J. Gowdy,[64] E. Grauges,[64] T. Haas,[64] T. Hadig,[64] V. Halyo,[64] T. Himel,[64] T. Hryn'ova,[64] M. E. Huffer,[64] W. R. Innes,[64] C. P. Jessop,[64] M. H. Kelsey,[64] P. Kim,[64] M. L. Kocian,[64] U. Langenegger,[64] D. W. G. S. Leith,[64] S. Luitz,[64] V. Luth,[64] H. L. Lynch,[64] H. Marsiske,[64] S. Menke,[64] R. Messner,[64] D. R. Muller,[64] C. P. O'Grady,[64] V. E. Ozcan,[64] A. Perazzo,[64] M. Perl,[64] S. Petrak,[64] B. N. Ratcliff,[64] S. H. Robertson,[64] A. Roodman,[64] A. A. Salnikov,[64] T. Schietinger,[64] R. H. Schindler,[64] J. Schwiening,[64] G. Simi,[64] A. Snyder,[64] A. Soha,[64] S. M. Spanier,[64] J. Stelzer,[64] D. Su,[64] M. K. Sullivan,[64] H. A. Tanaka,[64] J. Va'vra,[64] S. R. Wagner,[64] M. Weaver,[64] A. J. R. Weinstein,[64] W. J. Wisniewski,[64] D. H. Wright,[64] C. C. Young,[64] P. R. Burchat,[65] C. H. Cheng,[65] T. I. Meyer,[65] C. Roat,[65] R. Henderson,[66] W. Bugg,[67] H. Cohn,[67] J. M. Izen,[68] I. Kitayama,[68] X. C. Lou,[68] F. Bianchi,[69] M. Bona,[69] D. Gamba,[69] L. Bosisio,[70] G. Della Ricca,[70] S. Dittongo,[70] L. Lanceri,[70] P. Poropat,[70] L. Vitale,[70] G. Vuagnin,[70] R. S. Panvini,[71] S. W. Banerjee,[72] C. M. Brown,[72] D. Fortin,[72] P. D. Jackson,[72] R. Kowalewski,[72] J. M. Roney,[72] H. R. Band,[73] S. Dasu,[73] M. Datta,[73] A. M. Eichenbaum,[73] H. Hu,[73] J. R. Johnson,[73] R. Liu,[73] F. Di Lodovico,[73] A. Mohapatra,[73] Y. Pan,[73] R. Prepost,[73] I. J. Scott,[73] S. J. Sekula,[73] J. H. von Wimmersperg-Toeller,[73] J. Wu,[73] S. L. Wu,[73] Z. Yu,[73] and H. Neal[74]

(*BABAR* Collaboration)

[1]*Laboratoire de Physique des Particules, F-74941 Annecy-le-Vieux, France*
[2]*Università di Bari, Dipartimento di Fisica and INFN, I-70126 Bari, Italy*
[3]*Institute of High Energy Physics, Beijing 100039, China*
[4]*University of Bergen, Institute of Physics, N-5007 Bergen, Norway*
[5]*Lawrence Berkeley National Laboratory and University of California, Berkeley, California 94720*
[6]*University of Birmingham, Birmingham B15 2TT, United Kingdom*
[7]*Ruhr Universität Bochum, Institut für Experimentalphysik 1, D-44780 Bochum, Germany*
[8]*University of Bristol, Bristol BS8 1TL, United Kingdom*
[9]*University of British Columbia, Vancouver, British Columbia, Canada V6T 1Z1*
[10]*Brunel University, Uxbridge, Middlesex UB8 3PH, United Kingdom*
[11]*Budker Institute of Nuclear Physics, Novosibirsk 630090, Russia*
[12]*University of California at Irvine, Irvine, California 92697*
[13]*University of California at Los Angeles, Los Angeles, California 90024*
[14]*University of California at San Diego, La Jolla, California 92093*
[15]*University of California at Santa Barbara, Santa Barbara, California 93106*
[16]*University of California at Santa Cruz, Institute for Particle Physics, Santa Cruz, California 95064*
[17]*California Institute of Technology, Pasadena, California 91125*
[18]*University of Cincinnati, Cincinnati, Ohio 45221*
[19]*University of Colorado, Boulder, Colorado 80309*
[20]*Colorado State University, Fort Collins, Colorado 80523*
[21]*Technische Universität Dresden, Institut für Kern- und Teilchenphysik, D-01062 Dresden, Germany*
[22]*Ecole Polytechnique, LLR, F-91128 Palaiseau, France*
[23]*University of Edinburgh, Edinburgh EH9 3JZ, United Kingdom*
[24]*Elon University, Elon University, North Carolina 27244-2010*
[25]*Università di Ferrara, Dipartimento di Fisica and INFN, I-44100 Ferrara, Italy*
[26]*Florida A&M University, Tallahassee, Florida 32307*
[27]*Laboratori Nazionali di Frascati dell'INFN, I-00044 Frascati, Italy*
[28]*Università di Genova, Dipartimento di Fisica and INFN, I-16146 Genova, Italy*
[29]*Harvard University, Cambridge, Massachusetts 02138*
[30]*University of Iowa, Iowa City, Iowa 52242*
[31]*Iowa State University, Ames, Iowa 50011-3160*
[32]*Laboratoire de l'Accélérateur Linéaire, F-91898 Orsay, France*

[33]Lawrence Livermore National Laboratory, Livermore, California 94550
[34]University of Liverpool, Liverpool L69 3BX, United Kingdom
[35]University of London, Imperial College, London SW7 2BW, United Kingdom
[36]Queen Mary, University of London, E1 4NS, United Kingdom
[37]University of London, Royal Holloway and Bedford New College, Egham, Surrey TW20 0EX, United Kingdom
[38]University of Louisville, Louisville, Kentucky 40292
[39]University of Manchester, Manchester M13 9PL, United Kingdom
[40]University of Maryland, College Park, Maryland 20742
[41]University of Massachusetts, Amherst, Massachusetts 01003
[42]Massachusetts Institute of Technology, Laboratory for Nuclear Science, Cambridge, Massachusetts 02139
[43]McGill University, Montréal, Quebec, Canada H3A 2T8
[44]Università di Milano, Dipartimento di Fisica and INFN, I-20133 Milano, Italy
[45]University of Mississippi, University, Mississippi 38677
[46]Université de Montréal, Laboratoire René J. A. Lévesque, Montréal, Quebec, Canada H3C 3J7
[47]Mount Holyoke College, South Hadley, Massachusetts 01075
[48]Università di Napoli Federico II, Dipartimento di Scienze Fisiche and INFN, I-80126, Napoli, Italy
[49]University of Notre Dame, Notre Dame, Indiana 46556
[50]Oak Ridge National Laboratory, Oak Ridge, Tennessee 37831
[51]University of Oregon, Eugene, Oregon 97403
[52]Università di Padova, Dipartimento di Fisica and INFN, I-35131 Padova, Italy
[53]Universités Paris VI et VII, Lab de Physique Nucléaire H. E., F-75252 Paris, France
[54]Università di Pavia, Dipartimento di Elettronica and INFN, I-27100 Pavia, Italy
[55]University of Pennsylvania, Philadelphia, Pennsylvania 19104
[56]Università di Pisa, Scuola Normale Superiore and INFN, I-56010 Pisa, Italy
[57]Prairie View A&M University, Prairie View, Texas 77446
[58]Princeton University, Princeton, New Jersey 08544
[59]Università di Roma La Sapienza, Dipartimento di Fisica and INFN, I-00185 Roma, Italy
[60]Universität Rostock, D-18051 Rostock, Germany
[61]Rutherford Appleton Laboratory, Chilton, Didcot, Oxon OX11 0QX, United Kingdom
[62]DAPNIA, Commissariat à l'Energie Atomique/Saclay, F-91191 Gif-sur-Yvette, France
[63]University of South Carolina, Columbia, South Carolina 29208
[64]Stanford Linear Accelerator Center, Stanford, California 94309
[65]Stanford University, Stanford, California 94305-4060
[66]TRIUMF, Vancouver, British Columbia, Canada V6T 2A3
[67]University of Tennessee, Knoxville, Tennessee 37996
[68]University of Texas at Dallas, Richardson, Texas 75083
[69]Università di Torino, Dipartimento di Fisica Sperimentale and INFN, I-10125 Torino, Italy
[70]Università di Trieste, Dipartimento di Fisica and INFN, I-34127 Trieste, Italy
[71]Vanderbilt University, Nashville, Tennessee 37235
[72]University of Victoria, Victoria, British Columbia, Canada V8W 3P6
[73]University of Wisconsin, Madison, Wisconsin 53706
[74]Yale University, New Haven, Connecticut 06511

(Received 7 September 2002; published 5 March 2003)

We present a measurement of the branching fraction for the decay of the neutral B meson into the final state $J/\psi\pi^+\pi^-$. The data set contains approximately 56×10^6 $B\overline{B}$ pairs produced at the $\Upsilon(4S)$ resonance and recorded with the *BABAR* detector at the PEP-II asymmetric-energy e^+e^- storage ring. The result of this analysis is $\mathcal{B}(B^0 \to J/\psi\pi^+\pi^-) = (4.6 \pm 0.7 \pm 0.6) \times 10^{-5}$, where the first error is statistical and the second is systematic. In addition, we measure $\mathcal{B}(B^0 \to J/\psi\rho^0) = (1.6 \pm 0.6 \pm 0.4) \times 10^{-5}$.

DOI: 10.1103/PhysRevLett.90.091801 PACS numbers: 13.25.Hw, 11.30.Er, 12.15.Hh

In the standard model, the decay $B^0 \to J/\psi\rho^0$ can give rise to CP-violating asymmetries (directly and through B^0-$\overline{B}^0$ mixing) [1]. Therefore, it is interesting to study the decay mode $B^0 \to J/\psi\pi^+\pi^-$ to understand the $J/\psi\rho^0$ component in the final state. Since these decays are Cabibbo and color suppressed, they could be sensitive to non-standard-model processes contributing, for example, through penguin amplitudes. Large non-standard-model effects could cause the branching fraction to differ significantly from the standard model prediction of $\mathcal{B}(B^0 \to J/\psi\pi^+\pi^-) = (4.8 \pm 0.8) \times 10^{-5}$ [2]. This decay mode has not previously been observed. CLEO quotes an upper

limit of $\mathcal{B}(B^0 \to J/\psi\rho^0) < 2.5 \times 10^{-4}$ at the 90% confidence level [4]. Here we present the first measurement of $\mathcal{B}(B^0 \to J/\psi\pi^+\pi^-)$.

The data used in the present analysis were collected at the PEP-II storage ring with the *BABAR* detector, described in detail elsewhere [5]. Charged particles are detected, and their momenta measured, with a 40-layer drift chamber (DCH) and a five-layer silicon vertex tracker (SVT), both operating in a 1.5 T solenoidal magnetic field. Surrounding the DCH is a detector of internally reflected Cherenkov radiation (DIRC), and outside this is a CsI(Tl) electromagnetic calorimeter (EMC). The iron flux return of the solenoid is instrumented with resistive plate chambers (IFR). The data sample used for the analysis contains approximately 56×10^6 $B\overline{B}$ pairs, corresponding to a luminosity of 51.7 fb^{-1} recorded near the $\Upsilon(4S)$ resonance. An additional 6.4 fb^{-1}, recorded approximately 40 MeV below the $\Upsilon(4S)$ peak, were used to study continuum backgrounds.

Events containing $B\overline{B}$ pairs are selected based on track multiplicity and event topology [6]. At least three tracks are required to originate near the nominal beam spot, with polar angle in the range $0.41 < \theta_{\rm lab} < 2.54$ rad, transverse momentum greater than 100 MeV/c, and a minimum number of DCH hits used in the track fit. To reduce continuum background the ratio of the second to zeroth Fox-Wolfram moment, $R_2 = H_2/H_0$, is required to be less than 0.5. The sum of charged and neutral energy must be greater than 4.5 GeV in the laboratory frame. The primary vertex of the event must be within 0.5 cm of the average measured position of the interaction point in the plane transverse to the beam line.

The J/ψ is reconstructed in the e^+e^- and $\mu^+\mu^-$ final states. Electron candidates must satisfy the requirement that the ratio of calorimeter energy to track momentum lies in the range $0.75 < E/p < 1.3$, the cluster shape and size are consistent with an electromagnetic shower, and the energy loss in the DCH is consistent with that for an electron. If an EMC cluster close to the electron track is consistent with originating from a bremsstrahlung photon, it is combined with the electron candidate.

Muon candidates must satisfy requirements on the number of interaction lengths of IFR iron penetrated ($N_\lambda > 2$), the difference between the measured and expected interaction lengths penetrated ($|N_\lambda - N_\lambda^{\rm exp}| < 2$), the position match between the extrapolated DCH track and the IFR hits, and the average and spread of the number of IFR strips hit per layer.

Pion candidates are accepted if they originate from close to the beam spot and are not consistent with being a kaon. The algorithm uses dE/dx information from the SVT and DCH, and the Cherenkov angle and number of photons from the DIRC.

Tracks are required to lie in polar-angle ranges where particle identification efficiency is measured with known control samples. The allowed ranges correspond approximately to the geometrical acceptances of the EMC for electrons, the IFR for muons, and the DIRC for pions.

Identified electron and muon pairs are fit to a common vertex and must lie in the J/ψ invariant mass interval 2.95 (3.06) to 3.14 GeV/c^2 for the e^+e^- ($\mu^+\mu^-$) channel.

B^0 candidates are formed by combining a J/ψ candidate with a pair of oppositely charged pion candidates consistent with coming from a common decay point. We also require the vertex positions of the lepton and pion pairs to be consistent. Further selection requirements are made using two kinematic variables: the difference, ΔE, between the energy of the candidate and the beam energy $E_{\rm beam}^{\rm cm}$ in the center-of-mass frame and the beam-energy substituted mass, $m_{\rm ES} = \sqrt{(E_{\rm beam}^{\rm cm})^2 - (p_B^{\rm cm})^2}$. After applying the loose requirements $5.2 < m_{\rm ES} < 5.3$ GeV/c^2 and $|\Delta E| < 0.12$ GeV, approximately one-quarter of the events contain more than one B^0 candidate, from which we keep the one with the smallest $|\Delta E|$. The distribution of the candidates in ΔE and $m_{\rm ES}$ is shown in Fig. 1. For the final signal sample, we require $|m_{\rm ES} - 5279.0\ {\rm MeV}/c^2| < 9.9\ {\rm MeV}/c^2$ and $|\Delta E| < 39$ MeV, which correspond to 4σ and 3σ ranges in the resolutions for $m_{\rm ES}$ and ΔE. After all selection criteria have been applied, 213 events remain.

An unbinned, extended maximum-likelihood [7] fit is performed on the invariant mass distribution of the two pions for the selected events, to determine the various contributions to the $B^0 \to J/\psi\pi^+\pi^-$ events. We consider five categories: (i) $B^0 \to J/\psi\rho^0$ events; (ii) $B^0 \to J/\psi K_S^0 (K_S^0 \to \pi^+\pi^-)$ events; (iii) $B^0 \to J/\psi\pi^+\pi^-$ (non-ρ^0 signal) events;

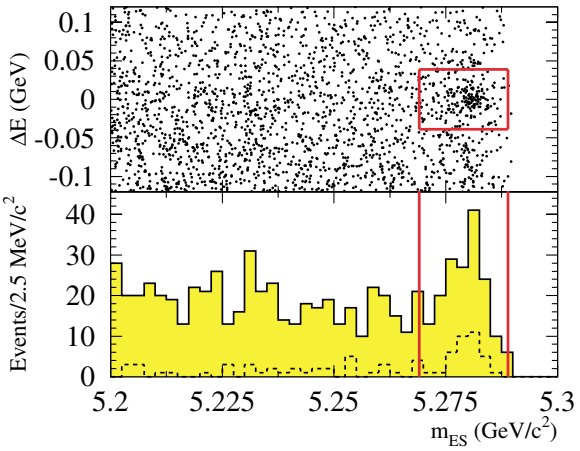

FIG. 1 (color online). Signal for $B^0 \to J/\psi\pi^+\pi^-$. The upper plot shows the distribution of events in the ΔE-$m_{\rm ES}$ plane, where the box represents the final selection criteria. The lower plot shows the distribution in $m_{\rm ES}$ of events with $|\Delta E| < 39$ MeV, where the dashed (solid) line corresponds to events in the K_S^0 (non-K_S^0) region in $M(\pi^+\pi^-)$ (0.45–0.55 GeV/c^2). The vertical lines represent the final selection.

(iv) background from events without a real J/ψ; and (v) inclusive-J/ψ background from events containing a real J/ψ. A probability density function (PDF) is constructed for each of these five cases. The total PDF is then formed from the sum of the five PDFs and fit to the data. The $B^0 \to J/\psi K^0_S$ mode is not considered to be a signal for the purposes of determining the branching fraction for $B^0 \to J/\psi\pi^+\pi^-$.

The PDF used to model the ρ^0 resonance in the $B^0 \to J/\psi\rho^0$ mode is a relativistic P-wave Breit-Wigner function [8]:

$$F_\rho(m) = [m\Gamma(m)P^{2L_{\rm eff}+1}]/[(m_\rho^2 - m^2)^2 + m_\rho^2\Gamma(m)^2],$$

where $\Gamma(m) = \Gamma_0(q/q_0)^3(m_\rho/m)[(1+R^2q_0^2)/(1+R^2q^2)]$. $q(m)$ is the pion momentum in the dipion rest frame, with $q_0 = q(m_\rho)$. $m \equiv M(\pi^+\pi^-)$ is the two-pion invariant mass and P is the J/ψ momentum in the B^0 rest frame. $m_\rho = 770\,\mathrm{MeV}/c^2$, $\Gamma_0 = 150\,\mathrm{MeV}/c^2$, and $m_\pi = 140\,\mathrm{MeV}/c^2$. $L_{\rm eff}$ is the effective orbital angular momentum between the J/ψ and the ρ^0, which can take any value between 0 and 2 and so is allowed to float in the fit. R is the Blatt-Weisskopf barrier-factor radius [9]. The fit is performed with R equal to two values (0.5 and 1.0 fm [10]) and the results of the two fits are averaged.

The PDF for the $B^0 \to J/\psi K^0_S$ mode is a single Gaussian function with the mass and width fixed to values obtained by fitting a sample of simulated $J/\psi K^0_S$ events. Allowing these parameters to vary in the final $M(\pi^+\pi^-)$ fit does not change the results.

The PDF used to model the $B^0 \to J/\psi\pi^+\pi^-$ (non-ρ^0 signal) contains a three-body phase-space factor $q(m)P(m)$ and a factor of $P(m)^2$ motivated by angular momentum conservation: $F_{\rm ph}(m) = q(m)P(m)^3$. If the $\pi^+\pi^-$ is in an S wave, angular momentum conservation results in a factor of $P(m)^2$, while a D wave yields a second power of $P(m)$ or higher. We choose to use the simple S wave for this PDF but take into account the possibility of a D-wave contribution by allowing an $f_2(1270)$ resonance in the fit as a systematic check.

The PDF for the $M(\pi^+\pi^-)$ distribution for background events without a real J/ψ is derived from a fake-J/ψ sample selected in data as described above except that at least one of the lepton candidates must fail the appropriate particle identification requirements. A Monte Carlo study confirms that the $M(\pi^+\pi^-)$ distribution obtained with this procedure correctly describes the shape of the non-J/ψ background. The resulting distribution is parametrized using the sum of two Weibull functions [11] and a Breit-Wigner. The Breit-Wigner describes the ρ^0 component of the non-J/ψ background.

The PDF for the $M(\pi^+\pi^-)$ shape for background events containing a real J/ψ is obtained from a simulated $B \to J/\psi X$ sample equivalent to a luminosity of 81 fb^{-1}. Events in which the system X is $\pi^+\pi^-$ (nonresonant), ρ^0, or K^0_S ($\pi^+\pi^-$) are removed from the sample. The resulting shape is described by a Weibull function.

The normalization of the background components is obtained from samples in data and simulation. The level of non-J/ψ background is obtained from sidebands of the J/ψ mass distribution in data. The $m_{\rm ES}$ distribution for these sideband candidates is then fit to an ARGUS function [12] to determine how many events pass the final selection criterion. Scaling to the equivalent background in the J/ψ mass region, using an exponential to describe the background shape in the J/ψ mass distribution, the expected non-J/ψ background is found to be 35.7 ± 1.2 events.

The level of inclusive-J/ψ background is obtained from the distribution of $m_{\rm ES}$ for events in the ΔE signal region in both data and simulation. In each case, the $m_{\rm ES}$ distribution is parametrized by a Gaussian function (to represent signal or peaking background) and an ARGUS function. Peaking background originates from $B \to J/\psi X$ decays such as $B \to J/\psi K^*$, $B^+ \to J/\psi\rho^+$, and $B \to J/\psi K_1$ that accumulate near $m_{\rm ES} = 5.279\ \mathrm{GeV}/c^2$.

The nonpeaking component of the inclusive-J/ψ background is determined by subtracting the non-J/ψ contribution, on the basis of the scaled sideband events described above, from the total ARGUS background in data. The peaking component is determined from the Gaussian part of the $m_{\rm ES}$ distribution in $B \to J/\psi X$ simulation, where events with $X = \pi^+\pi^-$ (nonresonant), ρ^0, and $K^0_S(\pi^+\pi^-)$ have been removed. The sum of peaking and nonpeaking components of the inclusive-J/ψ background is found to be 61 ± 11 events, of which the peaking component comprises six events. Thus, any associated uncertainties, such as branching fractions used in the $J/\psi X$ simulation, will not contribute significantly to the final systematic uncertainty.

The branching fraction is obtained from

$$\mathcal{B}(B^0 \to J/\psi\pi^+\pi^-) = \frac{N_{J/\psi\pi\pi}}{N_{B^0} \times \epsilon_{J/\psi\pi\pi} \times \mathcal{B}(J/\psi \to \ell^+\ell^-)}, \quad (1)$$

where $N_{J/\psi\pi\pi}$ is the total signal yield obtained from the fit, N_{B^0} is the total number of B^0 and $\overline{B}^0$ in the data sample [6], and $\epsilon_{J/\psi\pi\pi}$ is the signal efficiency. The J/ψ branching fraction $\mathcal{B}(J/\psi \to \ell^+\ell^-)$ is fixed to 11.81% [3]. We assume that the branching fraction for $\Upsilon(4S) \to B^0\overline{B}^0$ is one-half.

The signal efficiencies for all requirements apart from particle identification criteria are derived from simulation. Lepton and pion identification efficiencies are determined with samples of known muons, electrons, and pions in the data from the following processes: $\mu^+\mu^-\gamma$, $\mu^+\mu^-e^+e^-$, e^+e^-, $e^+e^-\gamma$, $D^{*+} \to D^0\pi^+$ ($D^0 \to K^-\pi^+$), and $K^0_S \to \pi^+\pi^-$. The efficiencies are determined as a function of momentum and polar and azimuthal angle. The typical average efficiencies (misidentification rates) for these particle identification algorithms are 97% (2%), 87% (7%), and 95% (5%) for

electrons, muons, and pions, respectively. The final signal efficiency of $(27.1 \pm 0.2)\%$ is the average of the $J/\psi\rho^0$ [$(27.1 \pm 0.3)\%$] and $J/\psi\pi^+\pi^-$ (nonresonant) [$(27.0 \pm 0.3)\%$] efficiencies, where the error is from Monte Carlo statistics.

A likelihood fit is performed on the $M(\pi^+\pi^-)$ distribution in data with the normalization of the non-J/ψ background fixed to 35.7 events and the inclusive-J/ψ background to 61. Thus, only the yields for $J/\psi\rho^0$, $J/\psi\pi^+\pi^-$ (non-ρ^0 signal), and $J/\psi K_S^0$ events are allowed to vary. The results of the fit are overlaid on the data points in Fig. 2. The goodness-of-fit χ^2 is 33.4 for 38 data points.

The result of the fit is 84 ± 13 signal events, of which 28 ± 10 are in the ρ^0 component and 55 ± 15 are in the non-ρ^0 signal component. The number of events in the K_S^0 component is 28 ± 5. Inserting the result into Eq. (1) yields the branching fraction $\mathcal{B}(B^0 \to J/\psi\pi^+\pi^-) = (4.6 \pm 0.7) \times 10^{-5}$, where the error is statistical.

The signal yield and statistical error can be checked by counting the number of events passing all the selection criteria and subtracting the estimated numbers of background and $J/\psi K_S^0$ events. This method gives 88 ± 15 $J/\psi\pi^+\pi^-$ events.

The systematic errors on the final branching fraction measurement arise from uncertainties on the signal efficiency, fitted yield, number of $B\overline{B}$ pairs produced, and $J/\psi \to \ell^+\ell^-$ branching fraction. $N_{B\overline{B}}$ is known to 1.1% with the dominant contribution to the uncertainty coming from the error on the $B^0\overline{B}^0$ selection efficiency. $\mathcal{B}(J/\psi \to \ell^+\ell^-)$ is known to 1.2% (fractional) [3].

The uncertainty on the pion identification efficiency is 1.8% per pion. Contributions to this error come from the limited size of the data sample used to determine the efficiency and the uncertainty on the kaon contamination in the sample. Uncertainties on electron and muon particle identification efficiencies come from studies using $B \to J/\psi X$ events in data. Fits to the $M(J/\psi)$ distribution in these events, under different selection criteria, give estimates of the electron and muon identification efficiencies and their errors, yielding an uncertainty of 1.3%.

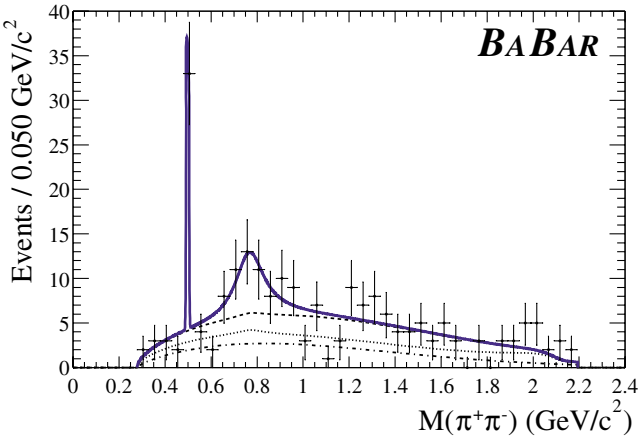

FIG. 2 (color online). Distribution of the invariant mass $M(\pi^+\pi^-)$ for events passing all selection criteria. The solid line is the result of the unbinned likelihood fit. The dashed line represents the sum of background and non-ρ^0 signal components. The dotted (dot-dashed) line shows the total (inclusive-J/ψ) background. The spike corresponds to $B^0 \to J/\psi K_S^0$ events.

The tracking efficiency uncertainty is 1.3% per track and is summed for the four tracks from the B^0 decay. The efficiency of the convergence requirement on the $\pi^+\pi^-$ vertex fit has been studied with a sample of $\psi(2S) \to \ell^+\ell^-$ decays; the associated uncertainty is 1%. The unknown ρ^0 helicity in the $J/\psi\rho^0$ component of the final sample introduces a systematic error on the efficiency of 2.5%. The limited amount of simulated data leads to an uncertainty in signal efficiency of 0.7%. To determine the effect of the signal and background shapes and the background yields on the fitted yields, the fixed parameters of these PDFs are varied within their uncertainties, allowing for correlations. This produces a total systematic error due to fit parameter variation of 9.7%, which is dominated by the errors in the background yields. The final fit neglects resonances such as $f_0(980)$, $f_2(1270)$, and $\rho^0(1450)$. Allowing for the addition of such terms in the likelihood function results in a systematic uncertainty on the yield of 2.1%. Varying the Blatt-Weisskopf radius between 0.5 and 1.0 fm gives no change in the total yield, while the variation of $L_{\rm eff}$ leads to a systematic uncertainty of 0.1%. The total fractional systematic uncertainty from all sources is found to be 12.3%.

The analysis is repeated with variations in the selection criteria. Taking into account statistical correlations between the results, we find that variations are consistent with statistical fluctuations due to the addition or removal of some of the events in the sample.

The branching fractions are measured separately for the modes $J/\psi \to e^+e^-$ and $J/\psi \to \mu^+\mu^-$ yielding the results $\mathcal{B}(B^0 \to J/\psi\pi^+\pi^-)_{ee} = (5.3 \pm 1.1) \times 10^{-5}$ and $\mathcal{B}(B^0 \to J/\psi\pi^+\pi^-)_{\mu\mu} = (4.0 \pm 1.0) \times 10^{-5}$, where the errors are purely statistical.

The $M(\pi^+\pi^-)$ distribution shows a clear peak at the ρ^0 mass. The fit result of 28 ± 10 events for the ρ^0 signal leads to a branching fraction of $\mathcal{B}(B^0 \to J/\psi\rho^0) = [1.6 \pm 0.6(\text{stat}) \pm 0.4(\text{syst})] \times 10^{-5}$. The systematic error includes a contribution from the effect of using an alternative PDF to describe the non-ρ^0 signal. The shape is from a polynomial fit to data recorded in π-π scattering experiments [13] and thus provides an empirically derived shape, in contrast to the default non-ρ^0 signal PDF, which is based on a phase-space assumption. The assumption that the non-ρ^0 signal is predominantly S wave, and therefore interference with the ρ^0 can be neglected, has been checked on data. A significant S-wave contribution means that the leptons from the J/ψ have a helicity angle distribution $\propto \sin^2(\theta_{J/\psi})$. For events in data with $M(\pi^+\pi^-) > 1.1$ GeV/c^2, we subtract the helicity cosine

distribution for events with $m_{\rm ES} < 5.27\ {\rm MeV}/c^2$ from the distribution for events in the signal $m_{\rm ES}$ region and find that the shape of the resulting distribution is consistent with $\sin^2(\theta_{J/\psi})$. Interference between S- and P-wave signal components integrates out in the $M(\pi^+\pi^-)$ projection, as long as the acceptance is symmetric in the cosine of the dipion helicity angle, $\theta_{\pi\pi}$. Studies using simulated nonresonant S-wave events show that there is no significant odd component to the acceptance function in $\cos(\theta_{\pi\pi})$. Consequently, there is no such interference contribution to the $\pi^+\pi^-$ mass distribution. The contribution to the fractional systematic uncertainty on $\mathcal{B}(B^0 \to J/\psi\rho^0)$ is 1.8% from varying the Blatt-Weisskopf radius and 3.3% from varying $L_{\rm eff}$.

In summary, the branching fraction for B^0 meson decay to the final state $J/\psi\pi^+\pi^-$ has been measured for the first time. The result, $\mathcal{B}(B^0 \to J/\psi\pi^+\pi^-) = [4.6 \pm 0.7({\rm stat}) \pm 0.6({\rm syst})] \times 10^{-5}$, is consistent with the standard model prediction [2]. In addition, the technique of fitting the $M(\pi^+\pi^-)$ distribution allows a measurement of the branching fraction for the $J/\psi\rho^0$ component. The result is $\mathcal{B}(B^0 \to J/\psi\rho^0) = [1.6 \pm 0.6({\rm stat}) \pm 0.4({\rm syst})] \times 10^{-5}$.

We are grateful for the excellent luminosity and machine conditions provided by our PEP-II colleagues and for the substantial dedicated effort from the computing organizations that support *BABAR*. The collaborating institutions thank SLAC for its support and kind hospitality. This work is supported by DOE and NSF (USA), NSERC (Canada), IHEP (China), CEA and CNRS-IN2P3 (France), BMBF and DFG (Germany), INFN (Italy), NFR (Norway), MIST (Russia), and PPARC (United Kingdom). Individuals have received support from the A. P. Sloan Foundation, Research Corporation, and Alexander von Humboldt Foundation.

*Also with Università di Perugia, I-06100 Perugia, Italy.

[1] I. Dunietz, H. R. Quinn, A. Snyder, W. Toki, and H. J. Lipkin, Phys. Rev. D **43**, 2193 (1991).

[2] The world average values [3] for the branching fractions $B^0 \to J/\psi K^{*0}$ and $B^0 \to J/\psi K^+\pi^-$ have been scaled by $0.5|V_{cd}|^2/|V_{cs}|^2$ and $|V_{cd}|^2/|V_{cs}|^2$, respectively. The number quoted in the text is the sum of the two scaled values and assumes that the tree amplitude is dominant.

[3] Particle Data Group, K. Hagiwara *et al.*, Phys. Rev. D **66**, 010001 (2002).

[4] CLEO Collaboration, M. Bishai *et al.*, Phys. Lett. B **369**, 186 (1996).

[5] *BABAR* Collaboration, B. Aubert *et al.*, Nucl. Instrum. Methods Phys. Res., Sect. A **479**, 1 (2002).

[6] For a description of the $B\overline{B}$ event selection, see, for example, Sec. VI of *BABAR* Collaboration, B. Aubert *et al.*, Phys. Rev. D **65**, 032001 (2002).

[7] R. J. Barlow, Nucl. Instrum. Methods Phys. Res., Sect. A **297**, 496 (1990).

[8] J. Pisut and M. Roos, Nucl. Phys. **B6**, 325 (1968).

[9] J. M. Blatt and V. F. Weisskopf, *Theoretical Nuclear Physics* (Wiley, New York, 1952), p. 361.

[10] Typical values of the Blatt-Weisskopf barrier-factor radius can be estimated from $q - \overline{q}$ meson models [see, for example, S. Godfrey and N. Isgur, Phys. Rev. D **32**, 189 (1985), especially Fig. 12] and from fits to experimental data [see, for example, D. Aston *et al.*, Nucl. Phys. **B296**, 493 (1988)].

[11] The Weibull function can be written as

$$W(m) = CV(m - M_{\rm on})^{(C-1)} \times \exp[-V(m - M_{\rm max})^C],$$

where $V = (C-1)/[C(M_{\rm max} - M_{\rm on})^C]$. $M_{\rm max}$ is the position of the function maximum, $M_{\rm on}$ is the lower kinematic cutoff, and C is a general shape parameter.

[12] ARGUS Collaboration, H. Albrecht *et al.*, Z. Phys. C **48**, 543 (1990).

[13] M. Gaspero, Nucl. Phys. **A562**, 407 (1993).